

## Kummer-function representation of ridge traveling waves

S. Watanabe

*Observatoire de Paris-Meudon, 92190 Meudon, France*

(Received 10 December 1986)

We present Kummer-function representation of an infinite set of local solutions for describing the double continua of two atomic electrons. Specific connection between the rate of flux loss from the ridge region and the double-excitation mechanism is discussed. Analysis based strictly on the local behavior of the solution leaves some ambiguity in threshold law for  $^3S^e$  and  $^1P^e$ ; otherwise Wannier's threshold law holds beyond reasonable doubt. The quantum-mechanical treatment is complemented and elucidated by classical trajectories.

### I. INTRODUCTION

The ionization cross section of an atom depends sensitively on the energy sharing between a pair of escaping electrons. Two-electron correlations thus attain a paramount importance near the double-ionization threshold. Wannier inferred that only a limited class of two-electron motion, confined to a neighborhood of the potential ridge,<sup>1-3</sup> results in double ionization, leading to the threshold law

$$\sigma \propto E^{1.13\dots} \quad (1)$$

The derivation of (1) by Wannier,<sup>1</sup> and Vinkalns and Gailitis<sup>2</sup> relied on classical trajectories and motivated critical examination using quantum mechanics.<sup>4,5</sup> This paper advances previous quantum treatments by providing Kummer-function representation of local ridge solutions.

The present treatment retains the concept of the effective potential energy considered by Macek<sup>6</sup> and Rau.<sup>4</sup> Its imaginary part relates the rate of flux loss from the ridge region and accounts for the double ionization and excitation mechanism, albeit qualitatively. This paper elucidates the double-excitation mechanism with the aid of the ridge solutions and displays of classical trajectories.

This paper is organized as follows, Section II A defines various quantities and concepts as a preparation for the discussions to follow. Section II B solves for the local ridge solutions in terms of Kummer's functions. We demonstrate in particular that the solution of Rau and Peterkop and that of Klar and Schlecht<sup>7</sup> are two members of a denumerably infinite family of local solutions. Section III presents classical trajectories representing double excitation, leading to the discussion of its mechanism and the connection with the intramolecular energy-transfer problem. Spin dependence of the threshold law relies on the scaling property of the wave packet propagating astride the ridge. Two cases are separately discussed. Section IV closes this paper with comments on remaining theoretical questions. Atomic units are used throughout.

### II. KUMMER-FUNCTION REPRESENTATION OF RIDGE SOLUTIONS

#### A. Preliminary discussion

The hyperspherical coordinates<sup>1,6-8</sup> are convenient for parametrizing the radial motion of the two electrons, par-

ticularly astride the ridge and orthogonally across it.<sup>3,9</sup> The radial distances  $r_1$  and  $r_2$  are reparametrized by

$$R = \sqrt{r_1^2 + r_2^2}, \quad (2a)$$

$$\alpha = \arctan \frac{r_1}{r_2}. \quad (2b)$$

Let us represent the wave function  $\Psi(\mathbf{r}_1, \mathbf{r}_2)$  as follows:

$$\Psi(\mathbf{r}_1, \mathbf{r}_2) = (R^{1/2} r_1 r_2)^{-1} F(R) \Phi(R; \alpha, \hat{\mathbf{r}}_1, \hat{\mathbf{r}}_2). \quad (3)$$

Although this has a form akin to the adiabatic channel representation of Macek,<sup>6</sup> we will not employ his adiabatic approximation in this paper. The Schrödinger equation for  $(R^{1/2} r_1 r_2) \Psi(\mathbf{r}_1, \mathbf{r}_2)$  is expressed in terms of the reduced Hamiltonian  $H$  given by

$$H = -\frac{1}{2} \frac{\partial^2}{\partial R^2} - \frac{1}{2R^2} \frac{\partial^2}{\partial \alpha^2} + \frac{T(\hat{\mathbf{r}}_1, \hat{\mathbf{r}}_2)}{2R^2} - \frac{1}{8R^2} + \frac{Z(\alpha, \theta_{12})}{R}, \quad (4)$$

where  $T(\hat{\mathbf{r}}_1, \hat{\mathbf{r}}_2)$  is the angular kinetic energy operator whose representation depends on the specific choice of a reference frame, and  $Z(\alpha, \theta_{12})$  is the effective charge given by

$$Z(\alpha, \theta_{12}) = R \left[ -\frac{z}{r_1} - \frac{z}{r_2} + \frac{1}{r_{12}} \right] \quad (5)$$

The ridge motion is characterized by its propagation near  $r_1 = r_2$  and  $\hat{\mathbf{r}}_1 = -\hat{\mathbf{r}}_2$ , namely, near the saddle point of the potential surface. Expanding  $Z(\alpha, \theta_{12})$  and  $T(\hat{\mathbf{r}}_1, \hat{\mathbf{r}}_2)$  about this point, we have

$$Z(\alpha, \theta_{12}) = Z_0 - \frac{v_1^2}{2} \beta^2 - \frac{v_2^2}{2} \gamma^2, \quad (6)$$

with

$$\begin{aligned} Z_0 &= \frac{(4z-1)}{\sqrt{2}} > 0, \\ v_1^2 &= \frac{(1-12z)}{\sqrt{2}} < 0, \\ v_2^2 &= \frac{1}{\sqrt{2}} > 0, \end{aligned} \quad (7)$$

as in Refs. 4 and 5, and  $T(\hat{\mathbf{r}}_1, \hat{\mathbf{r}}_2)$  is given by Eqs. (2-

4)-(2-6) of Nikitin and Ostrovsky.<sup>10</sup> In (6) and hereafter, we use the parameters

$$\beta = \frac{\pi}{4} - \alpha, \quad (8a)$$

$$\gamma = \frac{1}{2}(\pi - \theta_{12}). \quad (8b)$$

(N.B. Our definition of  $\gamma$  differs from Rau's by the factor of  $\frac{1}{2}$ .) The permutation symmetry of the two-electron wave function plays an important role at the saddle point, motivating the use of the body frame attached to the ridge configuration. We take as the  $z$  axis the interelectronic axis  $\hat{\mathbf{r}}_{12}$  which is a stable principal axis of inertia, and as the other two, the unit vectors parallel to  $\hat{\mathbf{t}} = \mathbf{r}_1 \times \mathbf{r}_2 / |\mathbf{r}_1 \times \mathbf{r}_2|$  and  $\hat{\mathbf{t}} \times \hat{\mathbf{r}}_{12}$ .<sup>11</sup> It is thus natural to represent  $\Phi(\mathbf{r}_1, \mathbf{r}_2)$  as

$$\Phi(\mathbf{r}_1, \mathbf{r}_2) = (\sin\theta_{12})^{-1/2} \sum_T \psi_T^{LS}(R, \alpha, \theta_{12}) D_{TM}^{L\eta}(\hat{\Omega}), \quad (9)$$

where  $L$  and  $S$  are the total angular momentum and spin. Here  $\hat{\Omega}$  represents the Euler angles of the transformation between the laboratory and body frames,  $T$  is the projection of  $\mathbf{L}$  onto the  $\hat{\mathbf{r}}_{12}$  axis, namely,  $T = \mathbf{L} \cdot \hat{\mathbf{r}}_{12}$ ,  $D_{TM}^{L\eta}(\hat{\Omega})$  is the molecular rotor function defined by

$$D_{TM}^{L\eta}(\hat{\Omega}) = \frac{1}{\sqrt{2}} [D_{TM}^{L\eta}(\hat{\Omega}) + \eta(-1)^T D_{-TM}^{L\eta}(\hat{\Omega})] \quad \text{if } L \neq 0 \quad (10)$$

$$= D_{TM}^{L\eta}(\hat{\Omega}) \quad \text{if } L = 0 \text{ and } \eta = +, ,$$

where  $\eta = \pi(-1)^L$ ,  $\pi$  being the parity under inversion, pertains to the parity under reflection with respect to the plane orthogonal to  $\hat{\mathbf{r}}_{12}$  at  $\alpha = \pi/4$ . We note the following symmetry properties<sup>11</sup> of  $\psi_T^{LS}$ :

$$\psi_T^{LS}(R, -\beta, \gamma) = \pi(-1)^{T+S} \psi_T^{LS}(R, \beta, \gamma), \quad (11a)$$

$$\psi_T^{LS}(R, \beta, -\gamma) = (-1)^{T-1/2} \psi_T^{LS}(R, \beta, \gamma), \quad (11b)$$

to be used in Sec. II B.

It is easy to verify that the Hamiltonian is diagonal in  $T$  at the ridge<sup>10</sup> and the Schrödinger equation is equivalent to

$$\left[ \frac{d^2}{dR^2} + k^2 - \frac{L(L+1) - T^2 - \frac{9}{4}}{R^2} + \frac{2Z_0}{R} - 2U(R) \right] \times F(R) = 0, \quad (12a)$$

$$\left[ \frac{\partial^2}{\partial R^2} + 2 \frac{d \ln F}{dR} \frac{\partial}{\partial R} + \frac{1}{R^2} \left[ \frac{\partial^2}{\partial \beta^2} - v_1^2 R \beta^2 \right] + \frac{1}{R^2} \left[ \frac{\partial^2}{\partial \gamma^2} - v_2^2 R \gamma^2 - \frac{T^2 - \frac{1}{4}}{\gamma^2} \right] \right] \psi_T^{LS} = -2U(R) \psi_T^{LS}, \quad (12b)$$

where  $U(R)$  is the effective potential energy akin in spirit to Macek's adiabatic one, although no adiabatic approximation is used here. Since the flux may get lost or gained in the ridge region depending on the coupling with other

modes,  $U(R)$  is complex valued in general,

$$U(R) = U_R(R) + iU_I(R). \quad (13)$$

A WKB-type approximation simplifies the representation of  $F(R)$  and of its logarithmic derivative<sup>3-5,12</sup> Consider now waves outgoing in  $R$ .  $F(R)$  may be written as

$$F^{(+)}(R) = \chi^{(+)}(R) \exp \left[ +i \int^R P(R') dR' \right], \quad (14)$$

where

$$P(R) = \left[ k^2 - \frac{L(L+1) - T^2 - \frac{9}{4}}{R^2} + \frac{2Z_0}{R} - 2U_R \right]^{1/2} \quad (15)$$

The Langer correction is not made here. Then  $\chi^{(+)}(R)$  satisfies

$$\frac{d^2 \chi^{(+)}}{dR^2} + 2iP(R) \frac{d\chi^{(+)}}{dR} + i \left[ \frac{dP}{dR} - 2U_I \right] \chi^{(+)} = 0. \quad (16)$$

The amplitude  $\chi^{(+)}(R)$  being a slowly varying function of  $R$ , we drop the term  $d^2 \chi^{(+)}/dR^2$ . Then

$$\chi^{(+)}(R) = P^{-1/2}(R) \tilde{\chi}^{(+)}(R), \quad (17)$$

with

$$\tilde{\chi}^{(+)}(R) = \exp \left[ \int^R [U_I(R')/P(R')] dR' \right], \quad (18)$$

which modifies the standard WKB amplitude due to the flux loss or gain since the exponent is equivalent to  $\int^t U_I(t') dt'$ ,  $P(R')$  being equal to the local velocity in a.u. We also have

$$\frac{d \ln F}{dR} = iP(R) + \frac{-\frac{1}{2} \frac{dP}{dR} + U_I}{P(R)}, \quad (19)$$

which is dictated by the first term when  $R$  is large. Hereafter, we retain terms of order  $1/R^{3/2}$  in the asymptotic expansion.<sup>4,5</sup>

## B. Kummer-function representation

We now solve for  $\psi_T^{LS}(R, \beta, \gamma)$  and  $U(R)$ , neglecting  $(\partial^2/\partial R^2) \psi_T^{LS}$  in comparison to  $2iP(R)(\partial/\partial R) \psi_T^{LS}$ . (This assumption can be checked *a posteriori*.) Let us introduce a pair of scaling functions  $v_1(R)$  and  $v_2(R)$  and an auxiliary function  $g^{(+)}(R, \beta, \gamma)$  through

$$\psi_T^{LS}(R, \beta, \gamma) = g^{(+)}(R, \beta, \gamma) f_1(x_1) f_2(x_2), \quad (20)$$

where

$$x_1 = v_1(R) \beta, \quad (21a)$$

$$x_2 = v_2(R) \gamma. \quad (21b)$$

It is easy to verify that the function  $f_j(x_j)$  satisfies the standard radial Schrödinger equation for the three-dimensional (anti)harmonic oscillator

$$\left[ \frac{d^2}{dx_j^2} - \bar{\nu}_j^2 x_j^2 - \frac{\lambda_j(\lambda_j + 1)}{x_j^2} \right] f_j(x_j) = -2\bar{\epsilon}_j f_j(x_j), \quad (22)$$

$$\begin{aligned} \lambda_1 &= 0, \\ \lambda_2 &= T - \frac{1}{2}, \end{aligned} \quad (22')$$

where the spring constant  $\bar{\nu}_j$  and energy of the oscillator  $\bar{\epsilon}_j$  are independent of  $R$  and are related to the potential energy  $U(R)$  by

$$U(R) = \frac{1}{R^2} [\bar{\epsilon}_1 v_1^2 + \bar{\epsilon}_2 v_2^2 + i \frac{1}{2} (A_1 + A_2)], \quad (23)$$

where  $A_j$  is a short-hand notation for

$$A_j = -R^2 P(R) \frac{d \ln v_j}{dR}, \quad (24)$$

which satisfies the equation

$$P(R) \frac{dA_j}{dR} + \frac{A_j^2}{R^2} + \frac{\nu_j^2}{R} = \bar{\nu}_j^2 \frac{v_j^4}{R^2} \quad (j=1,2). \quad (25)$$

The scaling factor  $g^{(+)}(R, \beta, \gamma)$  now reads

$$g^{(+)}(R, \beta, \gamma) = \exp\{i \frac{1}{2} [A_1(R)\beta^2 + A_2(R)\gamma^2]\}. \quad (26)$$

It is now necessary to solve Eq. (25) for  $v_j(R)$ . Letting

$$S_j(R) = A_j(R) - i \bar{\nu}_j v_j^2(R), \quad (27)$$

we find that  $S_j$  satisfies Eq. (15) of Peterkop.<sup>5</sup> The solution is reproduced in the Appendix for later reference. Let us solve for  $v_j^2(R)$  formally. Equations (24) and (27) reduce to an inhomogeneous first-order differential equation for  $v_j^{-2}(R)$ ; we get

$$v_j^{-2}(R) = 2i \bar{\nu}_j u_j^2(R) \int^R \frac{1}{R'^2 P(R') u_j^2(R')} dR' + B_j u_j^2(R), \quad (28)$$

where  $u_j(R)$  is defined by (A2') and  $B_j$  is an arbitrary constant which may depend on the nuclear charge.

There are two possible behaviors of  $v_j(R)$  corresponding to  $B_j=0$  and  $B_j \neq 0$ . One sees readily by substituting (A2') and (A3) into (25) that, for  $B_j \neq 0$ ,  $\bar{\nu}_j=0$  while for  $B_j=0$ ,

$$\bar{\nu}_j^2 = -\mu_j^2 \left[ \frac{Z_0}{2} \right], \quad (29)$$

where  $\mu_j$  is defined by (A5). For the  $\gamma$  mode one can see that by letting  $z \rightarrow \infty$  the separability of Eq. (12b) in this limit implies  $B_2 \neq 0$ . It is thus likely that the homogeneous solution  $B_2 \neq 0$  is important for the  $\gamma$  mode when  $z$  is finite. As for the  $\beta$  mode, it remains unclear which term should play the more dominant role since the Coulomb problem ( $z \rightarrow \infty$ ) including exchange is generally non-separable. Notice, however, that in the Coulomb zone  $v_1(R)$  behaves as  $R^{1/4}$  if  $B_1=0$  and as  $R^{1/4-\mu_1/2}$  if  $B_1 \neq 0$ . Since  $\frac{1}{4} - \mu_1/2$  is less than  $-1$ , the profile  $f_1(x_1)$  broadens as a function of  $\beta$  if  $B_1 \neq 0$ . This contradicts the intuitive picture of double ionization and excitation that the relevant configuration space shrinks as  $R$  increases. For this reason the case  $B_1=0$  appears more sensible al-

though there is no *a priori* reason to exclude the other possibility. We shall show in Sec. III B that except for the two symmetries  ${}^3S^e$  and  ${}^1P^e$  the threshold law is given by Eq. (1), regardless of whether  $B_1=0$  or not, provided that the radial motion is strongly unstable and the scaling function  $v_j(R)$  is real since this quantity has a direct correspondence with the classical trajectory with real energy. For the two exceptions it is necessary to know whether or not  $B_1=0$ . Let us note that  $f_j(x_j)$  may be expressed in terms of the regular spherical Bessel function when  $\bar{\nu}_j=0$ . We will not consider it separately since this case may be realized as the limit of  $\bar{\nu}_j \rightarrow 0$  in the Kummer-function representation to be provided below.

We are ready to discuss the behavior of  $f_j(x_j)$  of Eq. (22) exploiting Kummer's functions. It is easy to verify that, dropping the index  $j$  for brevity,

$$f(x) = x^{\lambda+1} e^{(1/2)\bar{\nu}x^2} N(x), \quad (30)$$

where  $N$  satisfies Kummer's differential equation

$$q \frac{d^2 N}{dq^2} + (\lambda + \frac{3}{2} - q) \frac{dN}{dq} - \frac{1}{2\bar{\nu}} (\bar{\epsilon} + \lambda + \frac{3}{2}) N = 0, \quad (31)$$

with

$$q = -\bar{\nu}x^2. \quad (32)$$

A solution which is finite at  $x=0$  and gives  $f(x)$  the parity  $(-1)^{\lambda+1}$  under  $x \rightarrow -x$  is

$$N \propto M \left[ \frac{\bar{\epsilon}}{2\bar{\nu}} + \frac{1}{2} \left[ \lambda + \frac{3}{2} \right], \lambda + \frac{3}{2}, q \right], \quad (33)$$

which is also commonly denoted as  $y_1$ .<sup>13</sup> Another solution which diverges as  $x^{-2(\lambda+1/2)}$  at  $x=0$  and gives  $f(x)$  the parity  $(-1)^{-\lambda}$  is

$$N \propto q^{-(\lambda+1/2)} M \left[ 1 + \frac{\bar{\epsilon}}{2\bar{\nu}} - \frac{1}{2} \left[ \lambda + \frac{3}{2} \right], -\lambda - \frac{1}{2}, q \right], \quad (34)$$

which is commonly denoted as  $y_2$ .<sup>13</sup> The second solution for  $f(x)$  resulting from (31) and (35) diverges at  $x=0$  unless  $\lambda \leq -\frac{1}{2}$ .

The asymptotic expansion of  $M(c, d, q)$  is necessary for imposing boundary conditions and to determine  $\bar{\epsilon}_j$ . As is well known,

$$\frac{M(c, d, q)}{\Gamma(d)} = \frac{e^{\pm i\pi c} q^{-c}}{\Gamma(d-c)} + \frac{e^q q^{c-d}}{\Gamma(c)}. \quad (35)$$

to the leading order when  $|q| \gg 1$ . Here the upper plus sign is taken if  $-\pi/2 < \arg(q) < 3\pi/2$ , and the lower minus sign, if  $-3\pi/2 < \arg(q) \leq -\pi/2$ .

### C. Quantization of the ridge mode for $B_j=0$

The spectrum of  $\bar{\epsilon}$  becomes quantized by boundary conditions at the limit of the ridge region where the ridge mode begins to couple with a large number of alternative ones. The nature of this coupling is discussed in Sec. III. To represent the coupling, we impose the following condition at large  $x_1$ : Only the outgoing wave in  $x_1$  has an ap-

preciable amplitude. In other words, the external region is highly absorptive.

Let us calculate the spectrum of  $\bar{\epsilon}_1$ . With the aid of Eq. (35), the instability of the radial motion expressed in the above-mentioned condition leads to

$$\bar{\epsilon}_1 = -i(n_1 + \frac{1}{2}) |\bar{v}_1| \quad (n_1 = 0, 1, 2, \dots) \quad (36)$$

The eigenfunction corresponding to  $n_1=0$  is identical to the local solution of Rau<sup>4</sup> and Peterkop,<sup>5</sup> and that corresponding to  $n_1=1$ , to that of Klar and Schlecht.<sup>7</sup>

Let us now consider the case where the absorptiveness of the space surrounding the ridge region is finite. Because we do not have specific knowledge of the behavior of the two electrons in the external space, this consideration is necessary for knowing how susceptible their behavior is to the change in the absorption coefficient. If it is too susceptible, we cannot circumvent a specific calculation of the modes prevalent outside the ridge. Friedman and Goebel<sup>14</sup> rewrite the eigenvalue equation for  $\bar{\epsilon}_1$  as

$$e^{iP(\bar{\epsilon}_1 + iA)} = \frac{\sqrt{2\pi} e^{(\pi/2)\bar{\epsilon}_1}}{(-\frac{1}{2} - i\bar{\epsilon}_1)!}, \quad (37)$$

where  $A$  is the absorption coefficient and  $P$  is the characteristic time of the antiharmonic oscillator in units of  $|\bar{v}_1|^{-1}$ , namely, the time of a trip from  $\beta=0$  to the limit of the ridge region and return. The value of  $P$  is large in our problem, the limit being at a great distance, and the velocity of the motion away from the ridge being small. Under this circumstance, one readily finds the following behavior of  $\bar{\epsilon}_1$ :<sup>14</sup> Spectrum (36) is valid up to  $n_1 \cong A$ . At  $n_1 > A$ ,  $\bar{\epsilon}_1$  acquires a real part while its imaginary part evolves very slowly. The lowest few values of  $\bar{\epsilon}_1$  are thus unaffected by the finite-absorption coefficient unless the ridge motion represents a *quasi-stable* periodic motion. This is not the case, as discussed in Sec. III. Spectrum (36) is therefore unaffected by the detail of the external region.

A few remarks before closing this section. Firstly, one can show that our wave function coincides with that of the product of outgoing spherical Coulomb wave functions at  $R = \infty$ , just as was done by Peterkop for the lowest solution. Secondly, the parity of  $\psi_T^{LS}$  under  $\beta \rightarrow -\beta$  is given by  $(-1)^{n_1}$ . This parity is denoted as  $A$  by Lin<sup>15</sup> and coincides with the phase in (11a). Equations (10) and (11a) make it evident that the two symmetries  ${}^3S^e$  and  ${}^1P^e$  cannot have  $A = +$  or  $n_1$ , even as noted by Greene and Rau<sup>16</sup> and Stauffer.<sup>17</sup> The limit  $\bar{v} \rightarrow 0$  obtains from Eq. 13.3.2 of Ref. 13, holding  $\bar{\epsilon}_j$  constant in (33) and (34). Owing to the fact that  $v_j(R)$  is real, the regularity condition on  $f(x)$  at  $x=0$  and  $x \rightarrow \infty$  leads to the fact that  $\bar{\epsilon}$  is real and non-negative. Thus, the  $\bar{\epsilon}$ -dependent term of  $U(R)$  is real when  $\bar{v}=0$ .

### III. PERIODIC TRAJECTORIES AND DOUBLE-EXCITATION PROCESS

#### A. Classical trajectories

This section aims at providing a physical picture of the excitation mechanism, whereby elucidating the role of the ridge traveling waves. For brevity, let us disregard the

detail of the angular correlation by constraining the electrons to move only along the  $x$  axis. Newton's equations read

$$p_i = \frac{dx_i}{dt}, \quad (38a)$$

$$\frac{dp_i}{dt} = -z \frac{x_i}{|x_i|^3} + \frac{x_i - x_j}{|x_i - x_j|^3}, \quad (38b)$$

where  $i \neq j = 1, 2$ . The result to be presented below has been obtained by the Runge-Kutta method and checked by the second-order predictor-corrector method. The conservation of the energy is satisfied to at worst one part in  $10^4$ . Let us first describe what types of periodic trajectories are present in this problem. Several examples are shown in Fig. 1 in the  $r_1$ - $r_2$  plane where  $r_i = |x_i|$ . Here  $z=1$  and the total energy  $E = -2.25 \times 10^{-4}$  a.u. This value of  $E$  corresponds to  $N=50$  in the double Rydberg formula of Read,<sup>18</sup>

$$E = -\frac{(z - \frac{1}{4})^2}{N^2}. \quad (39)$$

There are two elementary types of periodic trajectories, one unstable and the other less unstable (quasistable for contrast). (There are numerous periodic trajectories which visit the neighborhood of these elementary ones. They may be considered as representing the coupling of the elementary types of periodic motion.) The unstable trajectories are of the ridge type pertaining to radial excitation. Let us first explain these trajectories labeled  $s_1, s_2, \dots$ . Trajectory  $s_1$  represents the in-phase motion of the electrons. It starts from the origin with the initial condition  $p_1 = -p_2$  and always stays on the line  $r_1 = r_2$ ; it hits the turning line satisfying

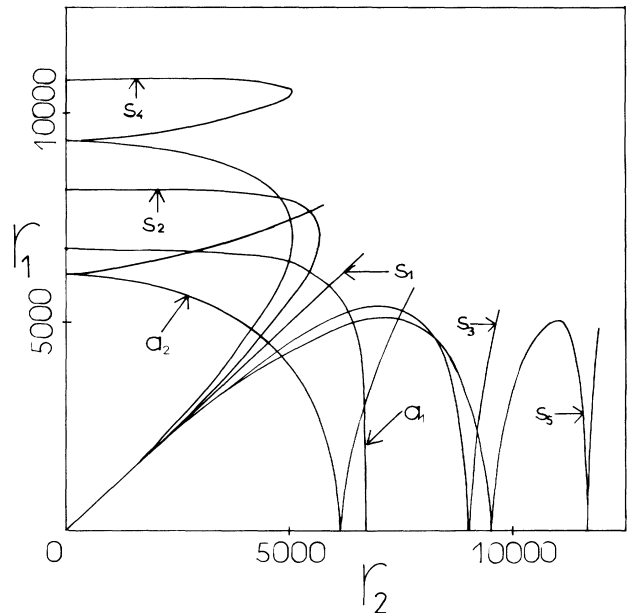


FIG. 1. Various periodic trajectories.  $s_1, s_2, \dots$ : unstable ridge-type trajectories.  $a_1, a_2$ : quasistable antisymmetric stretching trajectories.

$$E = -\frac{1}{r_1} - \frac{1}{r_2} + \frac{1}{r_1 + r_2}, \quad (40)$$

and then reverses itself toward the origin. This type of motion is known as the symmetric stretching mode in molecular physics. Trajectory  $s_2$  similarly starts from the origin but the initial magnitude of  $p_1$  and  $p_2$  is slightly different. At early times, the trajectory moves along the  $r_1 = r_2$  line but the disparity in velocity increases. In this figure, the velocity of electron 2 becomes zero before that of electron 1. Electron 2 then begins to fall toward the nucleus. When it reaches there and reverses the motion, electron 1 reaches the turning point and begins to fall toward the nucleus. The other trajectories  $s_3, s_4, \dots$ , can be interpreted in a similar fashion. When the trajectory begins to reverse itself, electrons 1 and 2 are in phase for  $s_1, s_3, \dots$ , while they are completely out of phase for  $s_2, s_4, \dots$ . There is an infinite number of such trajectories owing to the permanent dipole moment of the classical atom. These trajectories are unstable since a slight perturbation of the initial condition leads either to a violent collision of the two electrons near the nucleus as demonstrated in Fig. 2(a) or to double excitation, as will be discussed shortly.

The quasistable type consists of trajectories labeled  $a_1, a_2, \dots$  of which only two are shown. Trajectory  $a_1$  represents out-of-phase motion of the electron pair, pertaining to the repetitive energy exchange between them. This type of motion is known as the antisymmetric stretching mode in molecular physics. When electron 1 is at the nucleus, electron 2 is at the turning point and vice versa. It is easy to show that it exists at any energy. This trajectory is quasistable because a small perturbation leads to a quasiperiodic trajectory which stays near  $a_1$ . Figure 2(b) demonstrates this point. It corresponds to a collision of electron 1 with a highly excited hydrogen atom. Upon collision, the two electrons approach trajectory  $a_1$ . They stay there for seven periods, then electron 2 autodetaches. A somewhat more visual description is provided in Fig. 3, by a section of the phase space in the  $R$ - $P_R$  plane where  $P_R = dR/dt = p_1 \sin \alpha + p_2 \cos \alpha$ . The trajectory of Fig. 2(b) appears as an almost closed curve in the neighborhood of trajectory  $a_1$ . The success of Macek's adiabatic approximation for describing doubly excited states stems from this behavior. The somewhat wiggly movement of the trajectory at larger values of  $R$  reflects the well-known imperfection of the hyperspherical coordinates for representing the asymptotic motion of the electron pair where the independent particle coordinates  $r_1$  and  $r_2$  are more appropriate.<sup>19</sup> The other trajectories,  $a_2, \dots$ , can be interpreted similarly.

Let us now describe the process of double excitation on the basis of the preceding discussion. Figure 4 shows an illustrative trajectory. It originates from  $r_1 = r_2 = 1$  a.u. and moves almost parallel to the ridge-type periodic trajectories. It hits the caustic then bends toward  $r_1 = 0$ . Electron 2 has enough energy to move farther out but is short of the escape energy and gets reflected back from the caustic. The trajectory enters the resonance region; it exits into the region of the dipole field and rebounds into the resonance region again. It gets sent back to the asymptotic region and returns to the resonance region for

the third time. There is a violent collision between the electrons this time; electron 1 gets pulled back to the resonance region by the dipole field. It reenters the resonance region and gets sent back to the asymptotic region. Another violent collision kicks electron 1 out to infinity this time. The behavior of this illustrative trajectory at later times is stochastic in the sense that a small change in the initial condition leads to drastically different final be-

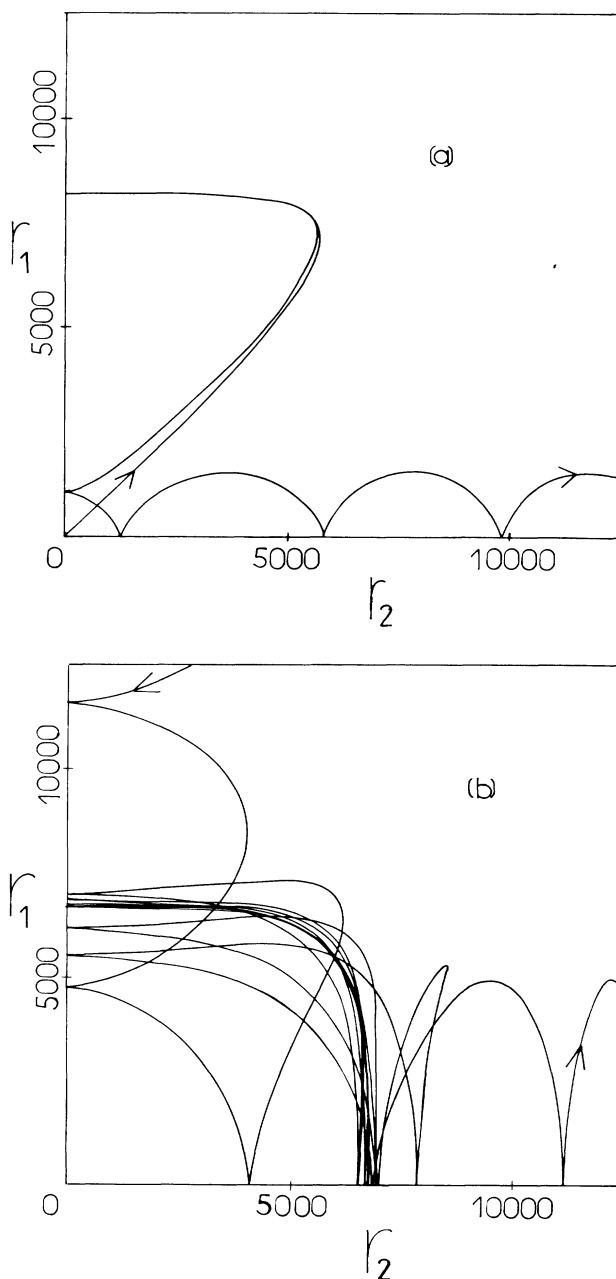


FIG. 2. (a) Evolution of a trajectory which comes close to trajectory  $s_2$  of Fig. 1. After bouncing back from the  $r_1$  axis, the two electrons experience a violent collision. (b) Evolution of a trajectory which comes close to a trajectory  $a_1$  of Fig. 1 at intermediate times. It bounces between the  $r_1$  and  $r_2$  axes seven times.

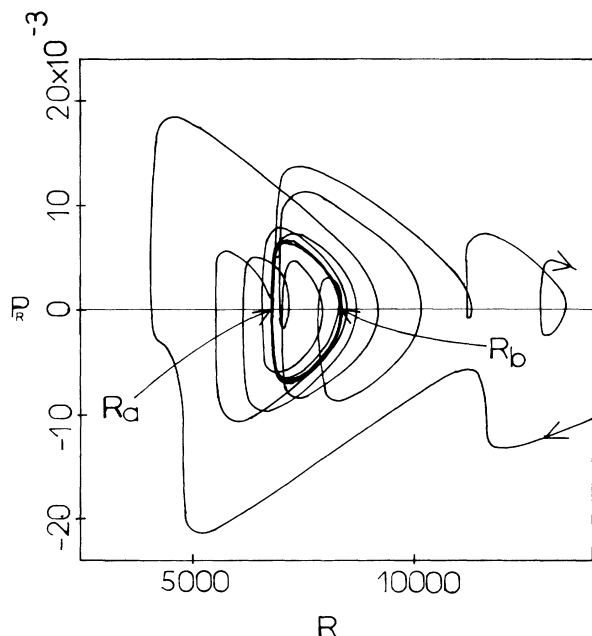


FIG. 3.  $R$ - $P_R$  phase-space section of the trajectory of Fig. 2(b). An almost closed curve appears near the center, representing quasiperiodic motion. This figure is suggestive of the success of Macek's adiabatic approximation.  $R_a$  and  $R_b$  are the turning points of the closed curve in this subspace.

havior. However, the energy distribution of the detached electron has a statistical significance.<sup>20</sup> One thing is clear, that in phase space most trajectories, resonant or non-resonant, will never return to the ridge trajectories within the characteristic time scale of the atomic system. The assumption regarding the large value of absorption coefficient  $A$  stems from this observation.

The initial point  $(r_1, r_2) = (1, 1)$  is merely representative of the target state  $H(1s)$ . Trajectories emanating from any other points in the charge cloud of  $H(1s)$  lead

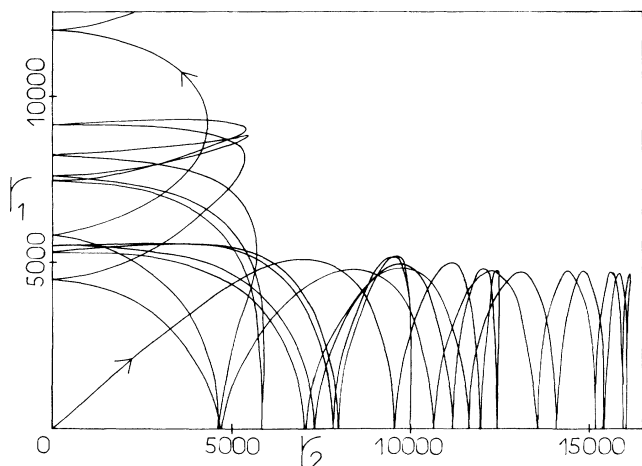


FIG. 4. An illustrative trajectory starting from  $(r_1, r_2) = (1, 1)$ . It evolves along the ridge at early times. At intermediate times it spends some time near trajectory  $a_1$  and some time in the dipole field of the classical atom. Electron 1 finally escapes.

to a similar conclusion. First, there is a characteristic ratio of  $p_1$  and  $p_2$  which makes a trajectory hit the caustic in the same way as trajectory  $s_1$ . When the ratio of the momenta is slightly superior or inferior to this, the trajectory enters the resonant region from either the lower half or the upper half of the  $r_1$ - $r_2$  plane. For judicious choice of  $p_1/p_2$ , the trajectory stays in the resonant region over several periods. The condensation point  $R_0$  marks the nearest approach of the trajectory to  $s_1$ , where the transverse velocity is zero. The value of  $R_0$  may be imaginary if the trajectory crosses  $s_1$ . For a given  $R_0$  there is an ensemble of points in the phase space representing various initial conditions for trajectories to start from within the  $H(1s)$  charge cloud. The local wave functions of Sec. II may be interpreted as a time-averaged representation of the corresponding wave packets.<sup>21</sup> A typical value of  $R_0$  is of the order of 100 a.u. which is larger than the size of  $H(1s)$  but rather small in comparison to the size of trajectory  $a_1$ , which is about 5000 a.u. Description of the two electrons by waves outgoing in the  $\beta$  mode applies at distances greater than  $R_0$ .

Before moving on to Sec. III B; a few remarks are in order. The behavior of the trajectory in Fig. 3 suggests that the resonance energy be attributed to the quasistable periodic trajectory rather than to the unstable ones,  $s_1, s_2, \dots$ . The double Rydberg formulas slightly modified to accommodate the variation in the screening constant of Eq. (39) reads<sup>18</sup>

$$E = -\frac{(Z - \sigma)^2}{N^2}. \quad (41)$$

When  $\sigma$  is evaluated using the quasistable periodic trajectory, it has a value between 0 and 0.25, the former corresponding to noninteracting electrons and the latter if they are rigidly located at  $r_1 = r_2$ . Because the electrons spend much time near the turning line close to  $r_1 = r_2$  where their motion is slow,  $\sigma$  is normally much closer to 0.25 than to 0 though generally inferior to 0.25. Indeed, most doubly excited intrashell states reveal this feature.<sup>11</sup>

Although the quasistable trajectory represents the out-of-phase motion of the two electrons, the corresponding wave function may be either symmetric (+type) or antisymmetric (-type) under the interchange of  $r_1$  and  $r_2$ . There is no conflict with the  $+/-$  classification of resonant states.

Quasistable periodic trajectories occur also in molecular reactive collisions such as  $FH + H$ .<sup>22</sup> Periodic trajectories topologically similar to  $s_1, s_2, \dots$  are found in the magnetic hydrogen problem.<sup>23,24</sup> However, there is no repulsive force near the nucleus in this case.

### B. Double excitation

This elucidates how the double excitation takes place quantum mechanically, exploiting the result of Sec. II and the physical picture provided by the classical trajectories. We make one major assumption: Trajectories moving initially close to the ridge-type trajectories *almost always* enter the resonance region, provided that they travel far enough to reach the neighborhood of the turning line.

Those trajectories which prematurely deviate from the ridge lead either to the elastic scattering or to the single excitation of the hydrogen atom without mediating the intermediate-resonant antisymmetric stretching mode. We italicized “almost always” because this assumption does not hold for certain values of  $p_1/p_2$  which lead to an immediate violent collision after reflecting back from the caustics, thus bypassing resonance. These values, however, occupy rather narrow windows in the phase space. Put differently, the phase-space density of the trajectories which will come close to trajectory  $a_1$  is expected to be high, thus insuring qualitative validity of the assumption. On the other hand, evaluation of the energy position of each resonant state and its width necessitates the knowledge of the system's behavior at the intermediate and later times so that an analysis based only on the early evolution of the ridge traveling waves would not be of use.

Let us impose the exponential decay condition on the  $R$ -mode wave function  $F^{(+)}(R)$  and on its complex conjugate. We readily find the WKB-type phase shift

$$\delta_{\text{WKB}} = \int_{R_{ii}}^{R_{ie}} P(R') dR' - i \int_{R_{ii}}^{R_{ie}} \frac{U_I(R')}{P(R')} dR' = 2N\pi, \quad (42)$$

where  $R_{ii}$  and  $R_{ie}$  are the interior and exterior turning points. (The Maslov indexes are dropped,  $N$  being large.) This quantization condition differs slightly from the usual one owing to the appearance of the even integer  $2N$ . This is because the state formed astride the ridge consists of a pair of electrons moving in phase, the factor 2 accounting for this fact.

Let us solve Eq. (42) for eigenenergies. Noting that the imaginary part is small compared to the real part, we may solve it iteratively. A single iteration gives the following quasibound state energy:

$$\epsilon_r = -\frac{Z_0^2}{8N^2} - i\frac{\Gamma}{2}, \quad (43)$$

where

$$\Gamma = 2\frac{Z_0^2}{8\pi N^3} \int_{R_{ii}}^{R_{ie}} \frac{U_I(R')}{P(R')} dR', \quad (44)$$

which is to be evaluated at  $\epsilon_r$ . (Note that the integrand is finite.) This width  $\Gamma$  is equal to the average of the imaginary part of the effective potential over one Kepler period of the electron pair because half the Kepler period of an electron moving in the field of an imaginary nucleus with the charge  $z^* = z - \frac{1}{4}$  is  $\tau_h = \pi N^3 / z^{*2} = 8\pi N^3 / z_0^2$ . Let us find the  $N$  dependence of  $\Gamma$ . This can be readily accomplished by introducing a new variable of integration

$$Q = \frac{ER}{Z_0}, \quad (45)$$

and using Eqs. (23), (24), and (28). The result is

$$\Gamma \propto N^{-3} \ln N, \quad (46)$$

whether or not  $B_j = 0$ .

The real part of  $\epsilon_r$  is a qualitative estimate of the quantized energy at which efficient energy transfer

should occur to all other unspecified modes at the rate given by  $2/\Gamma$ . The estimate is qualitative since it is equivalent to the quantized energy of trajectory  $s_1$  only and disregards energy distribution in the other neighboring trajectories. Nonetheless, this energy formula coincides with the double Rydberg formula with  $\sigma = \frac{1}{4}$ . As noted earlier, the resonance energy of an intrashell-type doubly excited state, namely, the quantized energy of an ensemble of trajectories near trajectory  $a_1$ , is given by the same formula (41), but with  $\sigma$  slightly different from  $\frac{1}{4}$ . Meanwhile the value of  $\Gamma$  is of the order of the energy spacing of a pair of doubly excited states in the neighboring  $N$  shells. Efficient energy transfer thus occurs from the ridge mode to the doubly excited states. This energy-transfer mechanism is analogous to the (1,1) resonance in molecular physics,<sup>21</sup> that is, rapid energy transfer occurs from the symmetric stretching mode to the antisymmetry stretching mode when they have nearly equal frequencies and when the symmetric stretching mode becomes quantum-mechanically unstable. Molecular states formed by this energy-transfer mechanism are analogous to the doubly excited states in atoms. A series of doubly excited states corresponding to an ensemble of trajectories which travel back and forth between the region of trajectory  $a_1$  and the asymptotic region (such as  $a_2$ ) appear as Feshbach or shape resonances. Excitation mechanism of such excited states is similar to that of the intrashell-type doubly excited states discussed above.

Let us now consider the energy dependence of the double-excitation cross section. The reader familiar with Wannier's theory of double ionization must have noticed that the assumption described in the first paragraph of this section sounds similar to his assumption that at energies slightly above the double-ionization threshold, trajectories reaching the asymptotic region  $Q \cong 1$ , lead to double ionization. This correspondence permits us to anticipate that the double-excitation cross section behaves just like the double-ionization cross section. Since our result in Sec. II is more general than the previous ones, let us outline the derivation.

An asymptotic observable requires one to define a wave function satisfying appropriate boundary conditions. This wave function is an incoherent superposition of local solutions obtained in Sec. II. Explicit connections between the initial ridge traveling waves and the final-state wave function thus necessitate a fuller knowledge than afforded by the local solutions. For the sake of brevity, let us ignore the incoherent sum for now and estimate the inelastic differential cross section for double excitation over an energy interval of order  $\Gamma$  mediated by a ridge traveling state labeled by the set of quantum numbers  $n_1, \bar{\epsilon}_2, T, L$ , and  $M$ ; we get

$$\frac{d\sigma}{d\theta_{12} d\hat{\Omega}} \propto |\tilde{\chi}_{n_1 \bar{\epsilon}_2}^{(+)}(R) f_{\bar{\epsilon}_2 T}(x_2) D_{TM}^{L\eta}(\hat{\Omega})|^2. \quad (47)$$

The phase-space volume available to the bundle of trajectories reaching the neighborhood of the turning line is  $P(R)$  due to the constraint  $\mathbf{p}_1 \cong -\mathbf{p}_2$ ,  $R$  being of the order of  $R_{ie}$ . This has canceled the WKB amplitude factor  $P^{-1}(R)$ . Using Eqs. (23), (24), (28), and (45), we find

$$\frac{d\sigma}{d\theta_{12}d\hat{\Omega}} \propto \begin{cases} |E|^{[(n_1+1/2)\mu_1-1/4]} |E|^{-(1/4)+|\text{Re}\mu_2|} |f_{\varepsilon_2 T}(x)D_{TM}^{L\eta}(\hat{\Omega})|^2 & \text{if } B_1=0, \\ |E|^{[\mu_1/2-1/4]} |E|^{-(1/4)+|\text{Re}\mu_2|} |f_{\varepsilon_2 T}(x)D_{TM}^{L\eta}(\hat{\Omega})|^2 & \text{if } B_1 \neq 0. \end{cases} \quad (48a)$$

$$\frac{d\sigma}{d\theta_{12}d\hat{\Omega}} \propto \begin{cases} |E|^{[(n_1+1/2)\mu_1-1/4]} & \text{if } B_1=0 \\ |E|^{[\mu_1/2-1/4]} & \text{if } B_1 \neq 0. \end{cases} \quad (48b)$$

(The condensation point  $R_0$  has been assumed to occur at a distance much smaller than  $R_{te}$ .) Integrating over angles, we get

$$\sigma \propto \begin{cases} |E|^{[(n_1+1/2)\mu_1-1/4]} & \text{if } B_1=0 \\ |E|^{[\mu_1/2-1/4]} & \text{if } B_1 \neq 0. \end{cases} \quad (49a)$$

$$\sigma \propto \begin{cases} |E|^{[(n_1+1/2)\mu_1-1/4]} & \text{if } B_1=0 \\ |E|^{[\mu_1/2-1/4]} & \text{if } B_1 \neq 0. \end{cases} \quad (49b)$$

Here the singular factor  $|E|^{-1/4+|\text{Re}\mu_2|}$  is canceled by the scaling factor  $|v_2(R_{te})| \propto |\Delta\theta_{12}|^{-1} \propto |E|^{-1/4+|\text{Re}\mu_2|}$ . If  $B_1=0$ , the double-excitation cross section should be dominated by the  $n_1=0$  component, except for the  $^1S^e$  and  $^1P^e$  symmetries. Thus for  $z=1$ ,  $\sigma \propto |E|^{1.13\dots}$  for all but the two exceptions for which the  $n_1=1$  component dominates, thus  $\sigma \propto |E|^{3.9\dots}$ , disregarding nonresonant excitation. If  $B_1 \neq 0$ , then the threshold law is independent of the nodal structure of  $f_1(x_1)$ . The classical experiment of Cvejanović and Read<sup>25</sup> supports Wannier's threshold law but shows a slight departure<sup>20,26</sup> at negative energies. The energy dependence of angular distribution, (48), is identical to that of Vinkalns and Gailitis.<sup>2</sup> Let us simply add that when  $\mu_2$  is purely imaginary the case  $B_2=0$  leads to the same threshold law as above.

Let us note that an efficient energy transfer should occur when the angular correlation pattern is preserved. The antisymmetric stretching mode would thus resonate when the correlation characterized by  $T$  is retained. If the two electrons do not lose memory of this correlation pattern during its exit into  $r_1$  or  $r_2 = \infty$ , the angular distribution following autodetachment should be given by

$$\frac{d\sigma}{d\theta_{12}d\hat{\Omega}} \propto |f_{\varepsilon_2 T}(x_2)D_{TM}^{L\eta}(\hat{\Omega})|^2. \quad (50)$$

The preservation of the angular correlation pattern characterized by  $T$  is known to hold well in the adiabatic treatment of the doubly excited states.<sup>11</sup> (This treatment amounts to freezing the symmetric stretching mode and averaging over the antisymmetric stretching mode as done for  $\text{H}_2\text{O}$  in molecular physics.<sup>27</sup>) An examination of the accurate calculation by Hyman *et al.*<sup>28</sup> indeed shows this to be true for the electron-impact ionization of  $\text{H}(1s)$  through the final  $\text{H}(2s,2p)+e$  channels with  $L=1$ , resonant energy transfer occurring by way of the intermediate antisymmetric stretching mode characterized by  $n_1=0$  and  $T=1$  which is also known as the  $+$  type channel.

Before closing this section, let us note that the cross section, Eq. (49), gives the double-ionization threshold law for positive values of  $E$ . The angular distribution given by Eq. (50) also holds well at  $E$  positive. The dynamically unfavored angular distribution studied by Greene<sup>29</sup> and Greene and Rau<sup>30</sup> for the photodetachment process

$$\text{H}^-(^1S^e) + h\nu \rightarrow \text{H}^+ + 2e^-, \quad (51)$$

with a linearly polarized photon, obtains immediately. Since  $T=1$ , for  $n_1=0, L=1, S=0$  and since  $M=0$ , we have

$$|D_{TM}^{L\eta}(\hat{\Omega})|^2 \propto \sin^2\theta, \quad (52)$$

where  $\theta$  is the angle between the  $z$  axes of the laboratory and body frames and  $\eta=+$ . The experimental circumstance identifies the  $z$  axis of the laboratory to be parallel to the polarization vector  $\hat{\varepsilon}$  whereas that of the body frame is parallel to  $\hat{r}_{12}$  hence the result. Physically, the final state represents a pair of electrons rotating about the axis. This axis is orthogonal to  $\hat{\varepsilon}$  by the dipole selection rule. The electrons escape retaining this geometry. This is an illustrative example of the usefulness of the molecular viewpoint.

#### IV. SUMMARY AND CONCLUSION

We deduced an infinite family of local solutions appropriate to describing wave propagation astride the ridge. The result is used to discuss the double-excitation process with the aid of classical trajectories. From the mechanical viewpoint, the double excitation occurs owing to the initial evolution of the system astride the ridge followed by the quasistable out-of-phase motion of the electron pair. Near threshold, the double-excitation cross section per unit energy interval depends on the energy just the way the double-ionization cross section does. However, a slight departure occurs possibly due to nonresonant processes.

Our treatment has centered on the wave packet propagating astride the ridge maintaining the profile given by  $f_j(x_j)$ . The two possible behaviors of the scaling function  $v_1(R)$  led to mutually exclusive results for the two symmetries  $^3S^e$  and  $^1P^e$ . The specification of  $v_1$  remained indeterminate in the present strictly local treatment.

We have not deduced the absolute total or differential cross sections. Let us mention that an attempt to deduce the absolute magnitude *ab initio* has been recently made by Crothers<sup>31</sup> applying a certain normalization procedure to a local solution.

Temkin and his collaborators<sup>32</sup> considered the modification of the Wannier threshold law by the Coulomb-dipole region of the configuration space. Critical examination of their theory lies outside the scope of the present analysis geared to the ridge region.

Although our treatment of Sec. II is largely quantum mechanical, it is not completely devoid of classical-mechanical aspects. The condensation point  $R_0$  which is equivalent to the integration constant  $c_1$  of the Appendix is a specific example. Since the propagator<sup>33</sup> has a more direct relationship with classical trajectories than does the



wave function, it appears of interest to reformulate the theory from such a point of view. In any event, no one has successfully constructed a fully quantum-mechanical ridge theory thus far. This is an open problem.

#### ACKNOWLEDGMENTS

The author thanks Professor U. Fano and Dr. Le Dourneuf for their continuing guidance. Valuable suggestions from Professor C. D. Lin and Dr. P. O'Mahony are gratefully acknowledged. Discussions with and numerous suggestions from Professor J. Macek helped clarify many questions. Preliminary computational investigations were carried out at the Centre Inter-Regional de Calcul Électronique in Orsay. Work supported in part by the ATP (Action Thématique Programmée) Physique Fondamentale of the Centre National de la Recherche Scientifique (CNRS) and in part by the North Atlantic Treaty Organization Grant No. 328. "Equipe de Recherche du CNRS No. 261" is a research group on the "Theory of Atomic and Molecular Processes at Low Energy" at the Observatoire de Paris-Meudon.

#### APPENDIX: ACTION FUNCTIONS

We may write

$$P(R) = [2(E + Z_0/R)]^{1/2} \quad (\text{A1})$$

to the order of  $R^{-3/2}$ .  $S_j(R)$  is given by

$$S_j(R) = R^2 P(R) \frac{d}{dR} \ln u_j(R), \quad (\text{A2})$$

$$u_j(R) = c_j u_j^{(1)} + u_j^{(2)}, \quad (\text{A2}')$$

where  $u_j^{(a)}(R)$  ( $a = 1, 2$ ) is given by

$$u_j^{(a)} = R^{m_{ja}} {}_2F_1 \left[ m_{ja}, m_{ja} + 1, 2m_{ja} + \frac{3}{2}, -\frac{ER}{2Z_0} \right] \quad (\text{A3})$$

and  $c_j$  is an arbitrary integration constant. Here the constants  $m_{ja}$  are given by

$$m_{ja} = \begin{pmatrix} -\frac{1}{4} + \frac{\mu_1}{2} & -\frac{1}{4} - \frac{\mu_1}{2} \\ -\frac{1}{4} + \frac{\mu_2}{2} & -\frac{1}{4} - \frac{\mu_2}{2} \end{pmatrix}, \quad (\text{A4})$$

where<sup>1,3,4</sup>

$$\begin{aligned} \mu_1 &= \frac{1}{2} \left[ \frac{100z - 9}{4z - 1} \right]^{1/2}, \\ \mu_2 &= \frac{1}{2} \left[ \frac{4z - 9}{4z - 1} \right]^{1/2}. \end{aligned} \quad (\text{A5})$$

Extension to  $E < 0$  involves one technical question, namely, the behavior of  $S_j(R)$  across the exterior turning point  $R_{te}$ . Fortunately, a useful set of connection formulas have been recently developed by Macek and Feagin.<sup>34</sup>

<sup>1</sup>G. H. Wannier, Phys. Rev. **90**, 817 (1953).

<sup>2</sup>I. Vinkalns and M. Gailitis, *Latvian Academy of Sciences, Report No. 4* (Zinantne, Riga, 1967), pp. 17–34; *Abstracts of the Fifth International Conference on the Physics of Electronic and Atomic Collisions, (ICPEAC), Leningrad, 1967*, edited by I. P. Flaks and E. S. Solov'ev (Nanka, Leningrad, 1967), p. 648.

<sup>3</sup>U. Fano, Phys. Rev. A **22**, 2660 (1980).

<sup>4</sup>A. R. P. Rau, Phys. Rev. A **4**, 207 (1971).

<sup>5</sup>R. Peterkop, J. Phys. B **4**, 513 (1971).

<sup>6</sup>J. H. Macek, J. Phys. B **1**, 831 (1968).

<sup>7</sup>H. Klar and W. Schlecht, J. Phys. B **9**, 1699 (1976).

<sup>8</sup>C. D. Lin, Phys. Rev. A **10**, 1986 (1974).

<sup>9</sup>U. Fano, Rep. Prog. Phys. **48**, 97 (1983).

<sup>10</sup>S. I. Nikitin and V. N. Ostrovsky, J. Phys. B **18**, 4349 (1985).

<sup>11</sup>S. Watanabe and C. D. Lin, Phys. Rev. A **34**, 823 (1986).

<sup>12</sup>J. M. Feagin, J. Phys. B **17**, 2433 (1984).

<sup>13</sup>*Handbook of Mathematical Functions*, Nat'l Bur. Stand. Appl. Math. Ser. No. 55, edited by M. Abramowitz and I. A. Stegun (U. S. GPO, Washington, DC, 1972), p. 504.

<sup>14</sup>W. A. Friedman and C. J. Goebel, Ann. Phys. **104**, 145 (1977).

<sup>15</sup>C. D. Lin, Phys. Rev. A **29**, 1019 (1984).

<sup>16</sup>C. H. Greene and A. R. P. Rau, Phys. Rev. Lett. **48**, 533 (1982).

<sup>17</sup>A. D. Stauffer, Phys. Lett. **91A**, 114 (1982).

<sup>18</sup>F. H. Read, J. Phys. B **10**, 449 (1977).

<sup>19</sup>B. L. Christensen-Dalsgaard, Phys. Rev. A **29**, 470 (1984).

<sup>20</sup>F. H. Read, J. Phys. B **17**, 3965 (1984).

<sup>21</sup>E. J. Heller, E. B. Stechel, and M. J. Davis, J. Chem. Phys. **73**, 4720 (1980).

<sup>22</sup>E. Pollak and M. S. Child, Chem. Phys. **60**, 23 (1981).

<sup>23</sup>M. A. Al-Laithy, P. F. O'Mahony, and K. T. Taylor, J. Phys. B **19**, L773 (1986).

<sup>24</sup>K. H. Welge (unpublished).

<sup>25</sup>S. Cvejanović and F. H. Read, J. Phys. B **7**, 1841 (1974).

<sup>26</sup>P. Hommand, F. H. Read, S. Cvejanović, and G. C. King, J. Phys. B **18**, L141 (1985).

<sup>27</sup>G. A. Natanson, G. S. Ezra, and G. Dalgado-Barrio, J. Chem. Phys. **84**, 2035 (1986); and (unpublished).

<sup>28</sup>H. A. Hyman, V. L. Jacobs, and P. G. Burke, J. Phys. B **5**, 2282 (1972).

<sup>29</sup>C. H. Greene, Phys. Rev. Lett. **44**, 869 (1980).

<sup>30</sup>C. H. Greene and A. R. P. Rau, J. Phys. B **16**, 99 (1983).

<sup>31</sup>D. S. F. Crothers, J. Phys. B **19**, 463 (1986).

<sup>32</sup>A. Temkin, Phys. Rev. A **49**, 365 (1982); A. Temkin, A. K. Bhatia, and E. Sullivan, Phys. Rev. **176**, 80 (1967); A. Temkin and Y. Hahn, Phys. Rev. A **10**, 708 (1974); A. Temkin, in *Electronic and Atomic Collisions*, edited by J. Eichler, I. V. Hertel, and N. Stolterfoht (Elsevier, New York, 1984), pp. 755–765.

<sup>33</sup>R. Balian and C. Bloch, Ann. Phys. **592** (1971); J. H. Macek (private communication).

<sup>34</sup>J. H. Macek and J. M. Feagin, J. Phys. B **18**, 2161 (1985).